Research Paper

A versatile supramolecular nanoadjuvant that activates NF-κB for cancer immunotherapy

Yan Xu[1], Youzhi Wang[3], Quanli Yang[1], Zhijia Liu[2], Zhiqiang Xiao[1], Zhicheng Le[2], Zhimou Yang[3,✉] and Chengbiao Yang[2,✉]

1. The First Affiliated Hospital, Biomedical Translational Research Institute and School of Pharmacy, Jinan University, Guangzhou 510632, China
2. School of Materials Science and Engineering, Center of Functional Biomaterials, Key Laboratory of Polymeric Composite Materials and Functional Materials of Ministry of Education, GD Research Center for Functional Biomaterials Engineering and Technology, Sun Yat-sen University, Guangzhou 510275, China
3. State Key Laboratory of Medicinal Chemical Biology, Key Laboratory of Bioactive Materials, Ministry of Education, College of Life Sciences, and Collaborative Innovation Center of Chemical Science and Engineering (Tianjin), Nankai University, Tianjin 300071, P. R. China

✉ Corresponding authors: Zhimou Yang, State Key Laboratory of Medicinal Chemical Biology, Key Laboratory of Bioactive Materials, Ministry of Education, College of Life Sciences, and Collaborative Innovation Center of Chemical Science and Engineering (Tianjin), Nankai University, Tianjin 300071, P. R. China. E-mail: yangzm@nankai.edu.cn or Chengbiao Yang, School of Materials Science and Engineering, Center of Functional Biomaterials, Key Laboratory of Polymeric Composite Materials and Functional Materials of Ministry of Education, GD Research Center for Functional Biomaterials Engineering and Technology, Sun Yat-sen University, Guangzhou 510275. E-mail: yangchb3@mail.sysu.edu.cn

Abstract

Although powerful adjuvants hold promise of vaccines for cancer immunotherapy, cumbersome preparation processes, elusive mechanisms and failure to induce T cell responses have largely limited their clinical translation. Due to their ease of synthesis, good biocompatibility and designable bioactivity, peptide derivatives-based supramolecular nanomaterials have attracted increasing interest in improving the immunogenicity of cancer vaccines.

Methods: Herein, we synthesized an NF-κB-activating supramolecular nanoadjuvant (3DSNA) that is prepared by pH-triggering self-assembly of a positively charged D-configurational peptide derivative. The immunostimulatory activity of 3DNSA was explored *in vitro* and *in vivo*.

Results: 3DSNA can strongly absorb the model antigen (ovalbumin, OVA) through electrostatic interaction. Then, 3DSNA promotes ingestion and cross-presentation of OVA, upregulation of costimulatory factors (CD80 and CD86) and secretion of proinflammatory cytokines (IL-6 and IL-12) by dendritic cells (DCs), accompanied by activation of the innate immune response (NF-κB signaling), resulting in long-term antigen-specific memory and effector CD8+ T cells response. When compared with conventional aluminum hydroxide adjuvant and the corresponding L-configurational supramolecular nanoadjuvant (3LSNA), 3DSNA-adjuvanted OVA (3DSNA+OVA) significantly prevents oncogenesis in naïve mice with a complete response rate of 60 %, restrains the tumor growth and prolongs the survival of melanoma-bearing mice.

Conclusion: These findings demonstrate that 3DSNA is a promising neo-adjuvant that enables various vaccines to be therapeutic for many important diseases including cancer.

Key words: Adjuvant, peptide self-assembly, immunotherapy, NF-κB activation, anti-cancer

Introduction

Successful cancer vaccines entail effective adjuvants to elicit a strong CD8+ T cell response [1-5]. Current adjuvants approved by the FDA, such as aluminum hydroxide and emulsion MF59, can only induce humoral immune response with little or no CD8+ T cell response. Therefore, there is a great research interest in developing neo-adjuvants that can initiate a robust CD8+ T cell response for cancer immunotherapy. To address this problem, various types of adjuvants, including liposomes [6, 7], poly (lactic-co-glycolic acid) [8-10], Au nanoparticles [11] and silica materials [12, 13] have been explored to

enhance antigen T-cells response. However, in the absence of immunomodulators (CpG, Poly (I:C), MPLA, etc.), few have the ability to coordinate optimal antigen presentation by antigen presenting cells (APC) with innate immune stimulation, which is critically important for inducing an effective CD8+ T cell response in the host. Moreover, the cumbersome preparation process of these formulations, involving chemical modification and an organic solvent, inevitably result in diminishing immunogenicity of antigens and the limitation of clinical application.

The supramolecular self-assembly process exists in nature and is closely related to the bioactivity of matter. Due to good manufacturing practices, biocompatibility and designable bioactivity, peptides have been used as building blocks to construct different supramolecular nanomaterials for drug delivery [14-17], cell cultures [17-20] and regenerative medicine [21, 22], *etc* [23-25]. In the field of immunomodulation, pioneering studies have demonstrated that supramolecular self-assembled nanomaterials based on peptides as adjuvants could greatly evoke an immune response in the host [26-30]. Recently, our studies [31, 32] have also shown that hydrogel formed by self-assembly of peptide derivatives with D-configuration amino acid could induce a strong antigen-specific humoral and cellular immune response, and the introduction of lysine (K) into the peptide derivative could further improve the immune response by promoting internalization of antigen by dendritic cells (DCs) [33]. Despite this progress, current strategies require covalent conjugation of antigen to materials and a heating-cooling cycle or enzymatic trigger process. Additionally, the mechanism of immune stimulation remained indistinct. These shortcomings impede the advanced development of peptide derivatives as vaccine adjuvant.

Aiming to develop a minimalist and versatile vaccine adjuvant with a clear mechanism of immune activation, we designed a series of peptide derivates with different amino acid configurations and numbers of lysine (K), Ada-G^{D}F^{D}F^{D}YG^{D}K$_n$-NH$_2$ (n = 1, 2, 3, named as 1D, 2D 3D) and Ada-GFFYGKKK-NH$_2$ (named as 3L) **(Figure S1-8)**.1-Adamantaneacetic acid (Ada) and FF were chosen due to their excellent ability to self-assemble, our recent study indicated that hydrogels based on the tetrapeptide GFFY showed powerful capabilities to activate immune response and were promising vaccine adjuvants [31] and K was used to absorb antigen through the charge-charge interaction and improve antigen immunogenicity. As illustrated in **Figure 1A**, compounds 2D, 3D and 3L could self-assemble into nanofibers at pH 7.4 in PBS buffer. Upon mixing with

the model antigens (OVA), these nanofibers could immediately capture the protein by charge interaction. Compared to the supramolecular nanoadjuvant formed by 2D (2DSNA) and 3LSNA, 3DSNA, as a desirable cancer vaccine adjuvant, could not only load antigen with high efficiency but also provoke a strong innate and adaptive immune response. Therefore, the configuration and number of K were critical for building powerful supramolecular nanoadjuvants to enhance the antigen-specific CD8+ T cell response in a facile and highly effective manner.

Materials and Methods

Materials

Fmoc-amino acids were bought from GL Biochem (Shanghai, CHN). PE-tagged 25-D1.16 monoclonal antibody that recognizes the SIINFEKL-H-2K^b complex, PE-tagged anti-CD86, APC-tagged anti-CD80, anti-MCHII-BV421, anti-CD86-APC, anti-IL-6-FITC, anti-IL-12-PE, Enzyme-linked immunosorbent assay (ELISA) kits for IL-6 and IL-12 were obtained from Biolegend (San Diego, USA). Alum adjuvant was acquired from Thermo Fisher (Waltham, USA). CpG adjuvant (ODN 1826) and chicken egg ovalbumin (OVA) were obtained from InvivoGen (Carlsbad, USA). Fluorescein and rhodamine-modified OVA were acquired from GenScript (Nanjing, CHN). Anti-CD8α tagged with APC, anti-IFN-γ tagged with FITC and anti-TNF-α tagged with PE were purchased from eBioscience (Waltham, USA). Chemical reagents and solvents were obtained from commercial sources without further purification.

Preparation of peptide derivates

Peptide derivates of Ada-G^{D}F^{D}F^{D}YG^{D}K-NH$_2$, Ada-G^{D}F^{D}F^{D}YG^{D}K^{D}K-NH$_2$, Ada-G^{D}F^{D}F^{D}YG^{D}K^{D}K^{D}K-NH$_2$, and Ada-GFFYGKKK-NH$_2$ were prepared by standard Fmoc solid-phase peptide synthesis (SPPS), as previously described.[33] In addition, the endotoxins of peptides < 1 EU mg^{-1} were measured by an endotoxin kit (Xiamen Bioendo Technology, CHN).

Preparation of nanofiber-adjuvants

Peptides (2 mg) were dissolved in 1 mL of 1x PBS buffer and 3 equiv. of Na$_2$CO$_3$ were used to adjust the pH value to 7.4. The solution was placed at room temperature for 12 h for molecular assembly.

Preparation of cancer vaccine formulated by nanofiber-adjuvants

Prefabrication nanofiber-adjuvant (1 mL) was mixed with 200 μg OVA power (endotoxin-free). The mixture stood at room temperature for 1 h to ensure sufficient absorption of the antigen.

Characterization of nanofiber-adjuvants and different vaccine formulations

The Zetasizer Nano ZS was used to measure the zeta potential of the nanoadjuvants and vaccine formulations at 25 °C in triplicate. Transmission electron microscope (TEM) was used to observe the morphology of the nanoadjuvants and vaccine formulations. For measurement of the loading efficiency of Rhod-OVA or protamine, vaccine formulated by nanofiber-adjuvant was centrifuged at 12000 rpm for 10 min; the optical density of supernatant was detected at 554 nm using a microplate reader for Rhod-OVA (Bio-RADiMark™, USA) or high performance liquid chromatogram (HPLC) for protamine.

Loading efficiency = $(1 - OD_{supernatant}/OD_{original})$ x 100 %

In vitro release of OVA from vaccine formulations

Triple vaccine formulations (1 mL) were incubated at 37 °C with continuous shaking at 150 rpm. The formulations were centrifuged at 12000 rpm for 10 min at the predetermined time point. All supernatants were removed and fresh PBS buffer was added into the vaccine formulations. The optical density of the supernatant was detected at 554 nm using a microplate reader.

In vitro cytotoxicity of nanofiber-adjuvants

Biocompatibility was evaluated by the Cell Counting Kit-8 (CCK-8) assay. Splenocytes were extracted from mouse spleen following the procedure described in previous reports [33]. In brief, at the pre-set time point, the spleen was collected and placed in RMPI1640 medium at 4 °C. The spleen was gently ground in stainless steel mesh. The solution was then filtrated in 200 mesh gauze to acquire monodisperse cell suspension. Cells were then seeded in 96-well plates at a density of 10^4 cells/well with a total medium volume of 200 μL. After 24 h, the cells were incubated with fresh cell medium containing nanofiber-adjuvants with serial concentrations operated by double dilution for 72 h, followed by the addition of 10 μL of CCK-8 reagent per well. Four hours later, cell viability was evaluated by using a microplate reader to measure the optical density at 450 nm.

BMDCs assays in vitro

Bone marrow cells were obtained from the femur and tibia of C57BL/6J mice. X-vivo 15 medium (Lanza, MD, USA) containing GM-CSF (20 ng/mL) and IL-4 (10 ng/mL) was used to culture the cells for 6 days. The culturing medium was replaced every two days. On day 7, 1 mL of culture medium per well containing $1×10^6$ BMDCs were seeded in 24-well plates; after 24 h, 50 μL formulated vaccines containing 100 μg nanofiber-adjuvants and 10 μg OVA, corresponding concentration of nanofiber-adjuvants or OVA were added to incubate for 24 h. Flow cytometry was performed to test BDMCs surface markers CD86 and CD80. ELISA kit and flow cytometry was carried out to determine the secreted IL-6 and IL-12 by BMDCs. Meanwhile, the BMDCs were collected to perform a western blot assay.

To evaluate the efficiency of nanoadjuvant on facilitating the internalization of antigen, 1 mL of culture medium per well containing $5×10^5$ BMDCs were seeded in 24-well plates and were incubated with 12.5 μL of vaccines containing 2.5 μg FITC-OVA and 25 μg nanofiber-adjuvant for 30 mins.

To analyze the intracellular location of p-p65, the activating form of NF-κB, the BMDCs were treated with OVA, 3LSNA, 3LSNA+OVA, 3DSNA, 3DSNA+OVA for 24h and cells treated with PBS were used as controls. The cells were washed twice with PBS, permeabilized with Triton X-100 (0.1 %) and fixed with paraformaldehyde (4 %), successively. The cells were then blocked with 2% BSA for 2h. Afterwards, they were incubated at 4 °C overnight with rabbit anti-p-NF-κB (anti-p-p65) primary antibody (1:100 dilution, Cell Signal Technology). The cells were washed and incubated with goat FITC-conjugated anti-rabbit IgG (1:500 dilution) for 1h. After washing with PBS, the cells were stained with undiluted Fluoroshield Mounting Medium with DAPI and analyzed by confocal microscopy.

To measure the cross-presentation of antigen, BMDCs were treated with OVA, CpG+OVA, 3LSNA+OVA, 3DSNA+OVA and PBS as a control. After incubation for 24 h, BMDCs were washed with PBS for three times. $1×10^5$ B3Z CD8C T hybridoma cells were incubated with $1×10^5$ treated BMDCs for another 24h in a 96-well plate. The medium was then removed and 150 μL detection buffer containing 0.15 mM chlorophenol red-β-D-galactopyranoside, 0.1% Triton X-100, 9 mM $MgCl_2$ and 100 μM mercaptoethanol was added. After incubation for 90 min at 37 °C, the 96-well plate was measured at 570 nm by a microplate reader. After incubation with D1.16 monoclonal antibody and MCH-II antibody for 30 min, the flow cytometry was carried out to measure the presentation.

Animal experiments

All work performed on animals was in accordance with and approved by the University Committee on Use and Care of Animals (UCUCA) at Sun Yat-sen and Jinan University. 6−8 weeks old female C57BL/6J mice were used for immune study

and tumor-bearing model building. 100 µL vaccine (containing 10 µg OVA and 100 µg nanofiber-adjuvant) were *s.c.* injected at the inguen of mice at designated time points. To analyze the OVA-specific CD8+ T cells, peripheral blood mononuclear cells (PBMCs) from vaccinated mice were stained with PE-tagged SIINFEKL-MHC tetramer (MBL, Japan) and APC-tagged CD8α antibody. To measure the antigen-specific CTLs, the PBMCs were collected and seeded in a 24-well plate with 1 mL per well containing 1×10^6 cells; 100 ng SIINFEKL per well was added to restimulate the PBMCs for 12 h, which were then stained with anti-CD8α tagged with APC, anti-IFN-γ tagged with FITC and anti-TNF-α tagged with PE. Here, 2×10^5 B16-OVA cells were *s.c.* injected on the right flank of mice for tumor therapy and 4×10^5 B16-OVA cells were *s.c.* inoculated for tumor prophylaxis; the tumor volume was calculated by the following equation: tumor volume = length × width^2 × 0.5. Animals were euthanized when the tumor volume reached more than 2000 mm^3.

Statistical Analysis

Data are shown as the means ± SEM in all graphs depicting error bars. The statistical significance of differences between experimental groups was determined by one-way ANOVA and two-way ANOVA using GraphPad Prism 7; P values are indicated by *, # and &.

Results and Discussion

Optimization of the number of lysine (K) in peptide derivatives for vaccine adjuvants

To explore the influence of K on adjuvant potency, the ability of these peptide derivatives to self-assemble was measured. We found that 2 mg/mL 1D resulted in precipitation after adjusting the PBS buffer to pH 7.4, which is similar to physiological conditions **(Figure S9)**, whereas 2 mg/mL 2D and 3D could self-assemble into homogeneously dispersed supramolecular nanofibers **(Figure 1B, C and Figure S9)**. However, there was no observed nanofibers when the pH value was adjusted to be 5.5 (Figure S10). When the number of K was 4, the peptide derivate could not self-assemble into nanofibers but nanoparticles **(Figure S11)**. Then, the ability of adjuvants to load antigen and stimulate immune responses was evaluated *in vitro*, as shown in **Figure 1E and 1F**. Compared with 2DSNA (96.1 and 93.6%, respectively), nearly 100 % (100.0 and 98.6 %, respectively) of the protein antigen was absorbed by 3DSNA at the weight ratio (OVA tagged with rhodamine, Rhod-OVA: DSNA) of 1:20 and 1:10.

When the weight ratio was 1:5 (Rhod-OVA: DSNA), the loading efficiency of 3DSNA also slightly exceeded that of 2DSNA. The zeta-potential results showed that 3DSNA without loading OVA possessed more surface positive charge than 2DSNA, and the value of both decreased with increased proportion of OVA. Moreover, compared to 2DSNA, which exhibited a surface negative charge at a weight ratio (Rhod-OVA: DSNA) of 1:5, 3DSNA still had a slight surface positive charge **(Figure 1G)**. Both 3DSNA and 2DSNA could not trap the protein (protamine) with a positive charge **(Figure S12)**. These results indicated that they interacted with the protein antigen through electrostatic absorption and therefore the loading efficiency of OVA by 3DSNA was higher than that by 2DSNA.

The stimulation of bone marrow dendritic cells (BMDCs) *in vitro* showed that both 2DSNA and 3DSNA significantly promoted the production and secretion of the proinflammatory cytokine IL-6 and IL-12 by BMDCs **(Figure 1H and 1I)**. More interestingly, 3DSNA significantly upregulated the expression of costimulatory CD80 and CD86 while 2DSNA failed to do so, implying that 3DSNA could induce a more potent immune response **(Figure 1J and 1K)**. These results indicated that the critical number of K in the peptide derivatives was three for endowing simultaneous formulation of vaccine and strong stimulation of immune response with high efficiency. Furthermore, 3L, used to study the effect of different configurations on adjuvant activity, could self-assemble into homogeneously disperse supramolecular nanofibers (3LSNA) **(Figure 1D and Figure S9)**, and then exhibited comparable results in terms of antigen loading and surface charge values **(Figure S13)** and the same morphology of nanofiber **(Figure S14)** as 3DSNA under the same prepared conditions. Therefore, 3DSNA and 3LSNA with good biocompatibility **(Figure S15)** were leveraged as adjuvants to formulate antigen into cancer vaccine (3DSNA+OVA and 3LSNA+OVA) for further study.

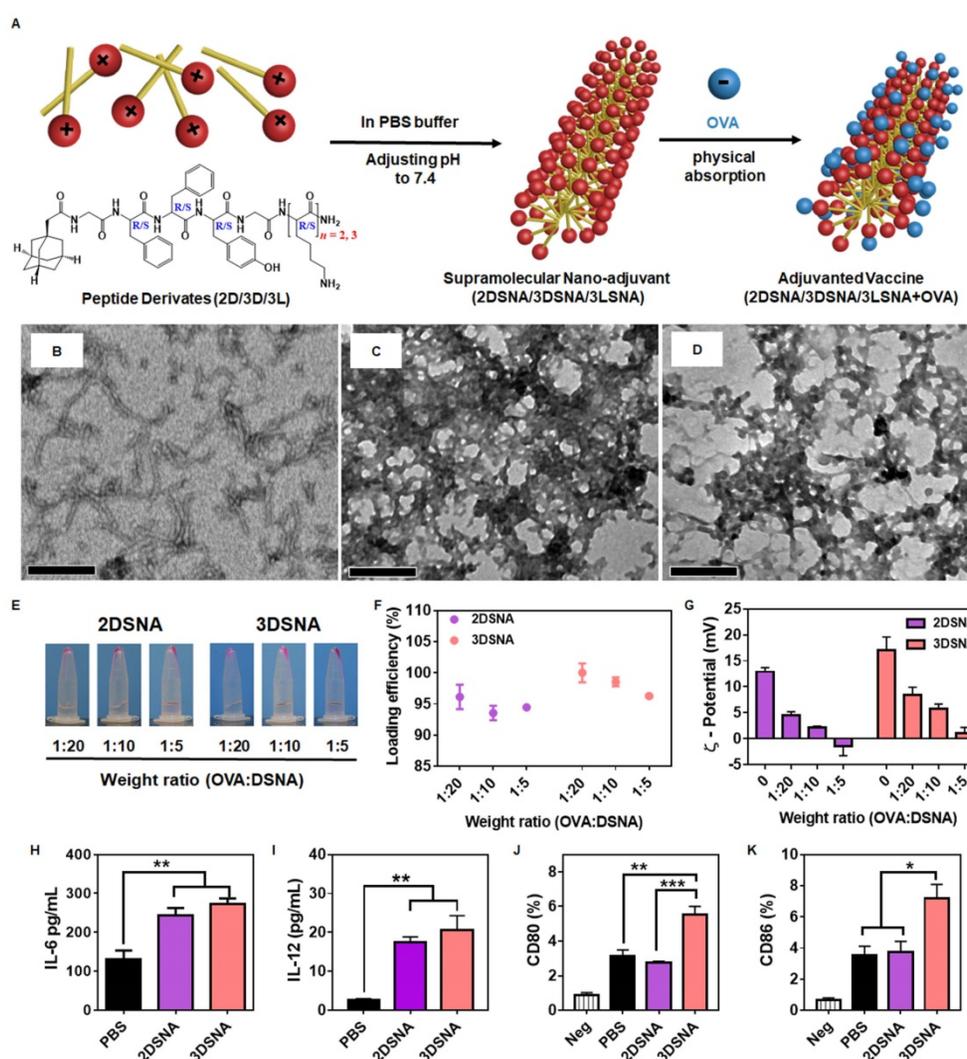### Vaccine formulated by 3DSNA protected the host against tumorigenesis

Naïve mice were vaccinated by subcutaneous (*s.c.*) injection of 3DSNA+OVA, 3LSNA+OVA, free OVA (OVA) and Alum+OVA on day 0 and 7 **(Figure 2A)**. On day 28, melanoma cells expressing OVA (B16-OVA) were used to challenge the vaccinated mice to explore the immune-stimulating capability of different vaccine formulations. Figure 2B showed that all mice immunized with OVA, Alum+OVA and 3LSNA+OVA suffered tumorigenesis after day 13 post-inoculation of tumor cells. The percentage of tumor-free mice was 60 % on day 35 post-inoculation

of tumor cells in the 3DSNA+OVA group, indicating vaccine adjuvanted by 3DSNA could effectively prevent the oncogenesis. On day 19 of post-injection of tumor cells, the average tumor volume only reached 49 mm³ in the 3DSNA+OVA group, which was significantly lower than that in the PBS (1571 mm³), OVA (1141 mm³), Alum+OVA (411 mm³), and 3LSNA+OVA (254 mm³) groups **(Figure 2C and 2D)**. After tumor cell challenge, the median survivals were 21, 21, 25 and 25 days in the PBS, OVA, Alum+OVA and 3LSNA+OVA groups, respectively, and it was encouraging that more than half (60 %) of the mice in the 3DSNA+OVA group still survived on day 35 **(Figure 2E)**. Since antitumor efficacy mainly depended on the cellular immune response, including cytotoxic T lymphocytes (CTLs), these results suggested that 3DNSA as an adjuvant possibly improved the cellular immune response to the OVA antigen.

3DSNA exhibited potent immunostimulatory behavior through activation of NF-κB

DCs, as unique APCs, play a key role in priming naïve T cells. To explore the mechanism of 3DSNA as a vaccine adjuvant to augment immune response for abolishing oncogenesis, the effects of 3DSNA on the kinetics of antigen and activity of DCs were studied. First, the release of antigen (Rhod-OVA) from 3DSNA+OVA and 3LSNA+OVA was monitored at pH conditions similar to the site of *s.c.* injection. **Figure S16** showed that Rhod-OVA could be released from both nanofibers over 192 h. The sustained release of OVA from both nanofibers favored slow clearance and degradation *in vivo*, improving the immunogenicity to some extent.
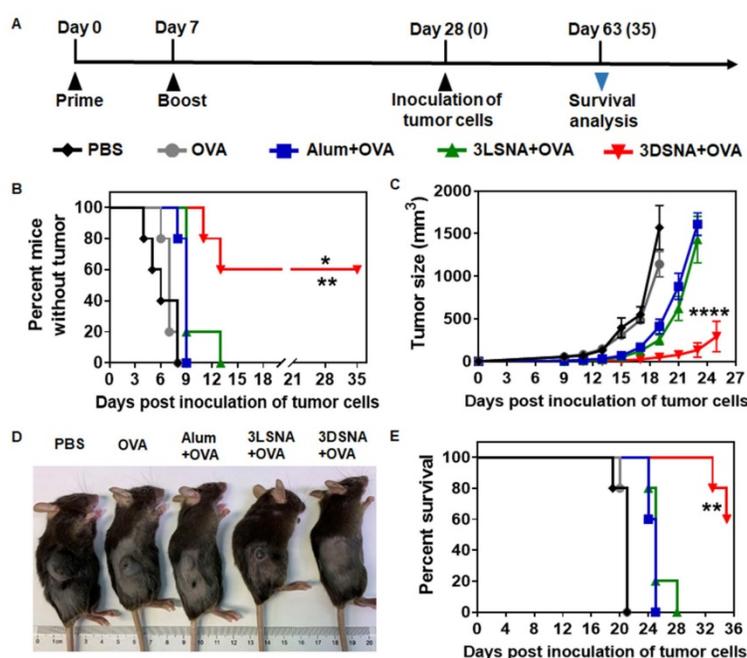

Figure 1. A) Schematic illustration of the preparation of supramolecular nanoadjuvant (2DSNA/3DSNA/3LSNA) and adjuvanted vaccine (2DSNA/3DSNA/3LSNA+OVA). The corresponding TEM images of **B)** 2DSNA, **C)** 3DSNA, **D)** 3LSNA. The scale bar was 500 nm. **E)** Optical pictures of OVA antigen absorbed by D-configurational supramolecular nanoadjuvant (DSNA), and **F)** corresponding loading efficiency of OVA at different weight ratios of OVA to DSNA. **G)** Zeta-potential of various formulations. **H)** IL-6 and **I)** IL-12 secreted by BMDCs after incubation with DSNA for 24 h (** $p < 0.01$, n = 3). **J)** CD80 and **K)** CD86 expressed by BMDCs after incubation with DSNA for 24 h (* $p < 0.05$, ** $p < 0.01$, *** $p < 0.001$, n = 3). The data were analyzed by one-way ANOVA.

Figure 2. A) Schematic of the immune study of naive mice. **B)** The percentage of vaccinated mice without tumorigenesis after challenge with B16-OVA cells on day 28; the data were analyzed by the log-rank test (** $p < 0.01$, 3DSNA+OVA compared with PBS, OVA, Alum+OVA; * $p < 0.05$, 3DSNA+OVA compared with 3LSNA+OVA, n = 5). **C)** Average tumor volume of vaccinated mice inoculated with B16-OVA cells on day 28; the data were analyzed by two-way ANOVA (**** $p < 0.0001$, 3DSNA+OVA compared with PBS, OVA, Alum+OVA and 3LSNA+OVA, n = 5). **D)** The representative pictures of tumor-bearing mice at day 18. **E)** The survival of vaccinated mice after inoculation with B16-OVA cells; the data were analyzed by the log-rank test (** $p < 0.01$, 3DSNA+OVA compared with PBS, OVA, Alum+OVA and 3LSNA+OVA, n = 5).

It was reported that cellular uptake of biologics could be improved by a nanomaterial-mediated endocytosis mechanism, hence the influence of nanofibers on antigen uptake by DCs was further investigated. Compared with the free OVA, both 3DSNA and 3LSNA exhibited a 1.5-fold higher cellular internalization of antigen (OVA tagged with FITC, FITC-OVA) into BMDCs **(Figure S17)**. The initiation of CD8+ T cell recognition of exogenous antigens demanded cross-presentation of internalized antigen. **Figure 3A and 3B** showed that 3DSNA+OVA, but not free CpG plus free OVA (CpG+OVA) or 3LSNA+OVA, significantly improved the cross-presentation of antigen by DCs compared with free OVA, which was mainly attributed to the possibility that there was a quicker release of antigen from 3DSNA+OVA (average rate = ~10 % per day) compared to the release from 3LSNA+OVA (~5 %), and 3DSNA+OVA accelerated antigen cross-presentation [34]. Costimulatory factors, CD86, and proinflammatory cytokines produced by DCs were considered as the second signal to activate the adaptive T cell response. The percentage of CD86-positive cells in BMDCs treated by 3DSNA+OVA was significantly higher than that in those treated with 3LSNA+OVA and 3LSNA, and slightly higher compared with free OVA and 3DSNA **(Figure S18A and S19)**. 3DSNA and 3DSNA+OVA potently facilitated the production of proinflammatory cytokines IL-6 **(Figure S18B)** and

IL-12 **(Figure S18C)**. Moreover, 3DSNA and 3DSNA+OVA enhanced the percentage of CD86+ IL-6+ **(Figure 3C and S20A)** and CD86+ IL-12+ **(Figure 3D and S20B)** cells among MCHII+ cells. These improvements could augment CD8+ T cell activation and differentiate CD8+ T cells into cytotoxic T lymphocytes (CTLs) [35, 36].

Previous studies have reported that NF-κB signaling is a pivotal mediator in the regulation of the innate and adaptive immune response [37-39]. The activity of this signal could promote antigen cross-presentation by MHC-I, costimulatory molecule upregulation, and proinflammatory cytokine production [40, 41]. To determine the molecular mechanism of adjuvant activity, the NF-κB signal pathway was measured by western blot assay. **Figure 3E** revealed that the levels of phosphorylation of p65 in the free OVA and 3LSNA groups were slightly higher than that in the PBS group, indicating that OVA and 3LSNA had a subtle influence on the activation of the NF-κB signal. The NF-κB signal was stronger in the BMDCs treated with 3LSNA+OVA than in those treated with OVA and 3LSNA, which probably resulted from their increased internalization of OVA. More importantly, 3DSNA and 3DSNA+OVA powerfully enhanced the phosphorylation of IKK-αβ, IkB-α and p65 in BMDCs compared with 3LSNA+OVA. Phosphorylation of IKK-αβ and IkB-α was slightly improved in the 3DSNA+OVA group, but p65 was not affected. The

LSCM results showed that the fluorescence signals of p-p65 in nucleus from both 3DSNA and 3DSNA + OVA-treated BMDCs were stronger than those in other group **(Figure 3F)**. These results indicated that 3DSNA dominated activation of canonical NF-κB signaling and had a strong function in enhancing the adaptive T-cell immune response. Given its immunostimulatory competence as well as its cost-effectiveness, 3DSNA could be recognized as the optimal adjuvant with the smallest number of lysines in this system.

3DSNA-adjuvanted vaccine induced strong antigen-specific CD8+ CTLs

To further validate whether antigen-specific CTLs were induced, naïve mice were primed by *s.c.* vaccination with different formulations on day 0, boosted on day 7, and then antigen-specific (SIINFEKL tetramer-recognizing) CD8+ T cells and IFN-γ or TNF-α secreting CD8+ T cells from peripheral blood mononuclear cells (PBMCs) were measured at the designated time point **(Figure 4A)**. 3DSNA+OVA powerfully increased the frequency of SIINFEKL-specific CD8+ T cells. The percentage of SIINFEKL+ CD8+ T cells among all CD8+ T cells peaked by 3.7 % after 1 week post final immunization, which was greater by 1.5, 1.4 and 1.3-fold compared with the values in the OVA, Alum+OVA and 3LSNA+OVA groups, respectively **(Figure 4B and 4C)**. On day 28, when the tumor cells were inoculated **(Figure 2A)**, the frequency was higher in

3DSNA+OVA (0.8 %) group than in the OVA (0.4 %), Alum+OVA (0.5 %) or 3LSNA+OVA (0.6 %) groups **(Figure S21 and S22)**. On day 28, the frequency of IFN-γ secretion by CD8+ T cells in the peripheral blood from mice treated with 3DSNA+OVA was 2.5-times higher than those treated with PBS. However, the frequency of IFN-γ+ CD8+ T cells in mice treated with Alum+OVA and 3LSNA+OVA were only approximately 1.5-times higher than PBS **(Figure 4D and S23)**. 3DSNA+OVA also significantly increased the production of CD8+ T cells secreting TNF-α **(Figure 4E and S23)**. These results implied that 3DSNA+OVA induced long-term strong antigen-specific memory and an effector CD8+ T-cells response, which was consistent with the strong efficacy of abrogating tumorigenesis **(Figure 2)** and would make for the suppression of tumor advancement.

3DSNA-formulated cancer vaccine effectively inhibited tumor growth

Female C57BL/6J mice (6-8 weeks) were used to establish a B16-OVA tumor-bearing model for evaluating the effect of tested vaccine formulations on tumor therapy **(Figure 5A)**. The day when tumor cells were inoculated *s.c.* was defined as day 0. At day 7, 14 and 21, the surviving mice were immunized respectively. The tumor size was monitored every two or three days. We found that vaccination with 3DSNA+OVA significantly delayed the tumor progression, which only reached ~ 175 mm^3 of tumor
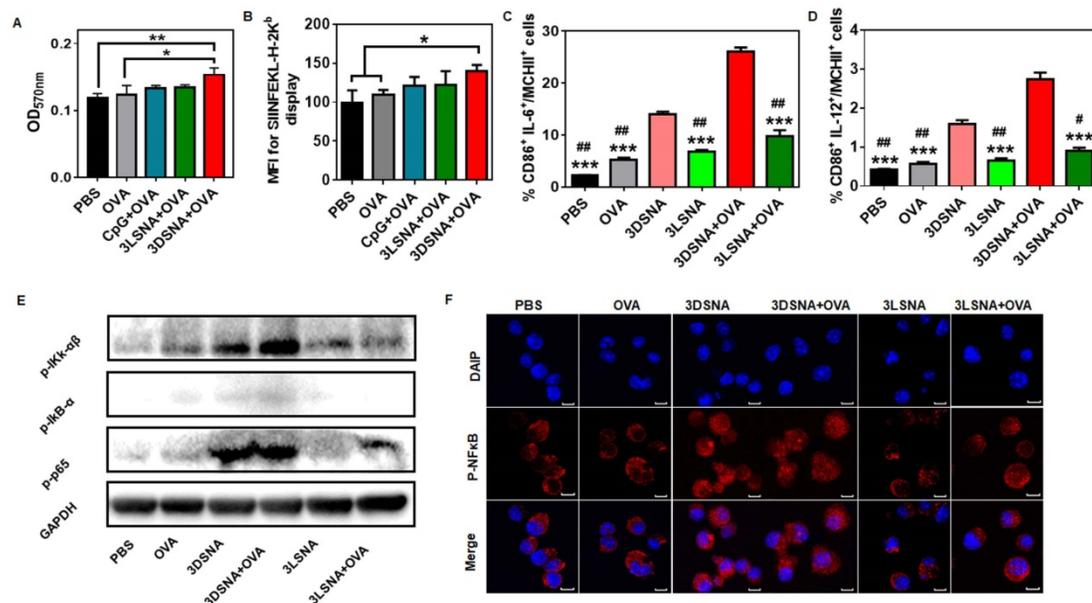

Figure 3. A) The cross-presentation of OVA by BMDCs after incubation with free OVA, CₚG+OVA, 3LSNA+OVA and 3DSNA+OVA for 24 h. **B)** The mean fluorescence intensity of presented SIINFEKL measured by flow cytometry. The percentage of **C)** CD86+ IL-6+ and **D)** CD86+ IL-12+ cells among MCH Ⅱ + cells (*** $p < 0.001$, 3DSNA+OVA compared with others, # $p < 0.05$, ## $p < 0.01$, 3DSNA compared with others, n = 3). **E)** Western blot of lysate from BMDCs treated with different formulations for 24 h. **F)** The analysis of p-p65 by laser scanning confocal microscopy. The data were analyzed by one-way ANOVA.

volume on day 21, whereas the tumor volume values were ~ 2158, 1460, 857 and 567 mm³ for the PBS, OVA, Alum+OVA and 3LSNA+OVA groups, respectively **(Figure 5B)**. As a result, the survival period for the tumor-bearing mice was substantially prolonged through vaccination with 3DSNA+OVA. Specifically, the median survival was 32.5 days for the 3DSNA+OVA group, which was an increase of approximately 67, 48, 38 and 25 % compared to the PBS, OVA, Alum+OVA and 3LSNA+OVA groups, respectively **(Figure 5C)**. This preferable anti-tumor activity could be accounted for the effector CD8⁺ T-cell response elicited by 3DSNA+OVA.

Conclusions

In this study, we have constructed a supramolecular nanoadjuvant (3DSNA) with good biocompatibility, which exhibited unique behaviors, including high antigen loading efficiency and improvement of the immune response against cancer vaccine. 3DNSA with nanofiber morphology is formed through self-assembly of a D-peptide derivative. This self-assembly is triggered by simply adjusting the pH, which involves no processes impairing antigen activity, such as chemical modification or the addition of exogenous enzyme or organic solvent. As a neo-adjuvant, it effectively binds with tumor antigen through simple electrostatic absorption, resulting in the increased expression of CD80 and CD86, production of IL-6 and IL-12, and cross-presentation of the SIINFEKL epitope by DCs in coordination with NF-κB activation. This delicate synchronization between cross-presentation of exogenous antigen and innate immunity stimulation initiates and develops naïve CD8⁺ T cells into antigen-specific CTLs secreting cytokines IFN-γ and TNF-α, which makes a vital difference in killing tumor cells **(Figure 5D)**. Although upstream targets of the NF-κB remains unknown, our study suggests that 3DSNA is an attractive candidate as adjuvant and suggest a general strategy in enhancing a range of subunit vaccines to elicit the CTL response for incurable diseases, including cancer.

Supplementary Material

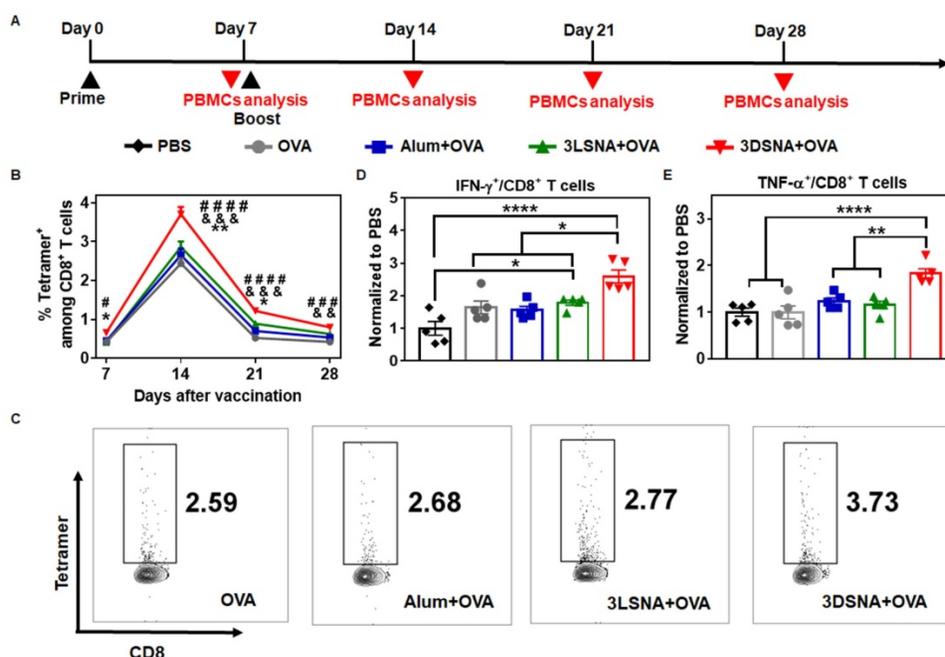Supplementary figures.
http://www.thno.org/v09p3388s1.pdf

Figure 4. A) Schematic of the immune study of naïve mice. **B)** The percentage of SIINFEKL⁺ among CD8⁺ T cells in peripheral blood on days 7, 14, 21 and 28 (& $p < 0.05$, && $p < 0.01$, &&& $p < 0.001$, 3DSNA+OVA compared with AlV; ## $p < 0.01$, ### $p < 0.001$, #### $p < 0.0001$, 3DSNA+OVA compared with OVA; * $p < 0.05$, ** $p < 0.01$, 3DSNA+OVA compared with 3LSNA+OVA). **C)** Representative flow cytometry dot plots for the frequency of SIINFEKL⁺ among CD8⁺ T cells in peripheral blood. After restimulation of PBMCs by SIINFEKL on day 28, the percentage of **D)** IFN-γ⁺ and **E)** TNF-α⁺ among CD8⁺ T cells was analyzed by flow cytometry (* $p < 0.05$, ** $p < 0.01$, *** $p < 0.001$, **** $p < 0.0001$, n = 5). The data were analyzed by one-way ANOVA.
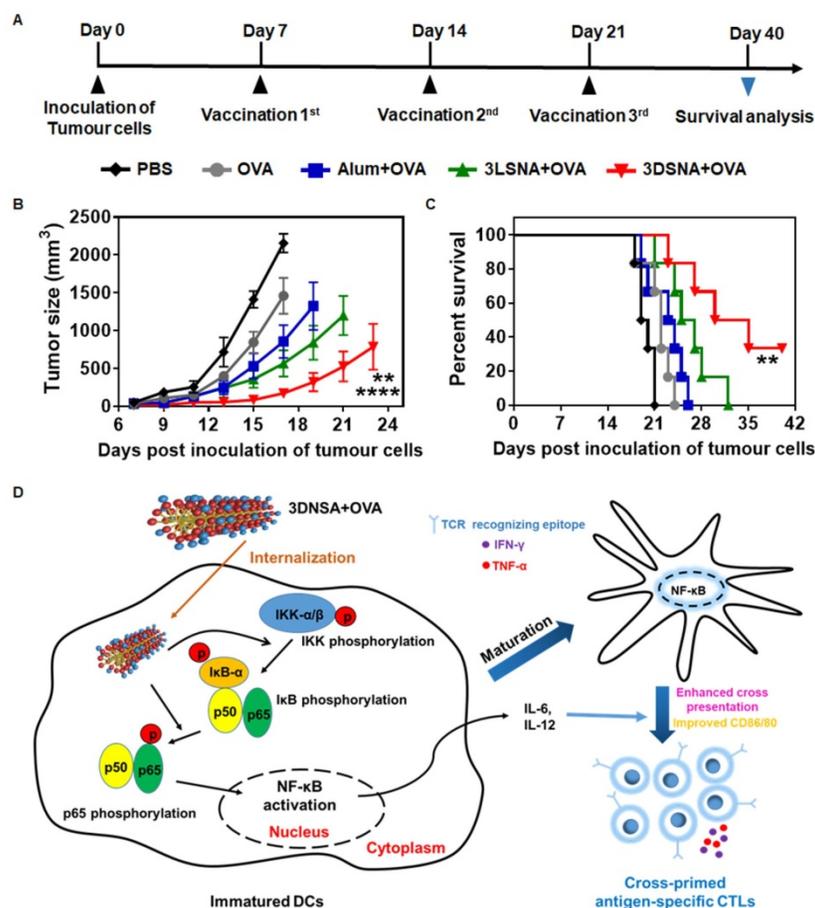
Figure 5. A) Schematic of the immune study of tumor-bearing mice. **B)** Average tumor volume in tumor-bearing mice vaccinated by different formulations; the data were analyzed by two-way ANOVA (**** $p < 0.0001$, 3DSNA+OVA compared with PBS, OVA, Alum+OVA; ** $p < 0.01$, 3DSNA+OVA compared with 3LSNA+OVA, n = 6). **C)** The survival of tumor-bearing mice treated with different formulations after tumor challenge; the data were analyzed by the log-rank test (** $p < 0.01$, 3DSNA+OVA compared with PBS, OVA and Alum+OVA, n = 6). **D)** Schematic of 3DSNA as versatile adjuvants initiating antigen-specific CTL responses for cancer immunotherapy.

Competing Interests

The authors have declared that no competing interest exists.

References

1. Fu J, Kanne DB, Leong M, et al. STING agonist formulated cancer vaccines can cure established tumors resistant to PD-1 blockade. Sci Transl Med. 2015; 7: 283ra52.
2. Melero I, Gaudernack G, Gerritsen W, et al. Therapeutic vaccines for cancer: an overview of clinical trials. Nat Rev Clin Oncol. 2014; 11: 509.
3. Reed SG, Orr MT, Fox CB. Key roles of adjuvants in modern vaccines. Nat Med. 2013; 19: 1597.
4. Romero P, Banchereau J, Bhardwaj N, et al. The Human Vaccines Project: A roadmap for cancer vaccine development. Sci Transl Med. 2016; 8: 334ps9.
5. Scheiermann J., Klinman DM. Clinical evaluation of CpG oligonucleotides as adjuvants for vaccines targeting infectious diseases and cancer. Vaccine. 2014; 32: 6377.
6. Huang W-C, Deng B, Lin C, et al. A malaria vaccine adjuvant based on recombinant antigen binding to liposomes. Nat Nanotechnol. 2018; doi: 10.1038/s41565-018-0271-3.
7. Sahin U, Derhovanessian E, Miller M, et al. Personalized RNA mutanome vaccines mobilize poly-specific therapeutic immunity against cancer. Nature. 2017; 547: 222.
8. DeMuth PC, Garcia-Beltran WF, Ai-Ling ML, Hammond PT, Irvine DJ. Composite Dissolving Microneedles for Coordinated Control of Antigen and Adjuvant Delivery Kinetics in Transcutaneous Vaccination. Adv Funct Mater. 2013; 23: 161-72.
9. Kroll AV, Fang RH, Jiang Y, et al. Nanoparticulate Delivery of Cancer Cell Membrane Elicits Multiantigenic Antitumor Immunity. Adv Mate. 2017; 29: 1703969.
10. Liu Q, Chen X, Jia J, et al. pH-Responsive Poly(d,l-lactic-co-glycolic acid) Nanoparticles with Rapid Antigen Release Behavior Promote Immune Response. ACS Nano. 2015; 9: 4925-38.
11. Niikura K, Matsunaga T, Suzuki T, et al. Gold Nanoparticles as a Vaccine Platform: Influence of Size and Shape on Immunological Responses in Vitro and in Vivo. ACS Nano. 2013; 7: 3926-38.
12. Li AW, Sobral MC, Badrinath S, et al. A facile approach to enhance antigen response for personalized cancer vaccination. Nat Mater. 2018; 17: 528-34.
13. Mahony D, Cavallaro AS, Stahr F, Mahony TJ, Qiao SZ, Mitter N. Mesoporous Silica Nanoparticles Act as a Self-Adjuvant for Ovalbumin Model Antigen in Mice. Small. 2013; 9: 3138-46.
14. Lyu L, Liu F, Wang X, et al. Stimulus-Responsive Short Peptide Nanogels for Controlled Intracellular Drug Release and for Overcoming Tumor Resistance. Chem Asian J. 2017; 12: 744-52.
15. Abbas M, Zou Q, Li S, Yan X. Self-Assembled Peptide- and Protein-Based Nanomaterials for Antitumor Photodynamic and Photothermal Therapy. Adv Mater. 2017; 29: 1605021.
16. Yu Z, Xu Q, Dong C, et al. Self-Assembling Peptide Nanofibrous Hydrogel as a Versatile Drug Delivery Platform. Cur Pharm Design. 2015; 21: 4342-54.
17. Wu C, Hu W, Wei Q, et al. Controllable Growth of Core&Shell Nanogels via Esterase-Induced Self-Assembly of Peptides for Drug Delivery. J Biomed Nanotechnol. 2018; 14: 354-61.
18. Roberts JN, Sahoo JK, McNamara LE, et al. Dynamic Surfaces for the Study of Mesenchymal Stem Cell Growth through Adhesion Regulation. ACS Nano. 2016; 10: 6667-79.
19. Wang H, Shi J, Feng Z, et al. An in situ Dynamic Continuum of Supramolecular Phosphoglycopeptides Enables Formation of 3D Cell Spheroids. Angew Chem Int Ed. 2017; 56: 16297-301.
20. Zhang S, Gelain F, Zhao X. Designer self-assembling peptide nanofiber scaffolds for 3D tissue cell cultures. Semin Cancer Biol. 2005; 15: 413-20.
21. Boekhoven J, Stupp SI. Supramolecular Materials for Regenerative Medicine. Adv Mater. 2014; 26: 1642-59.
22. Pugliese R, Gelain F. Peptidic Biomaterials: From Self-Assembling to Regenerative Medicine. Trends Biotechnol. 2017; 35: 145-58.

23. Amit M, Yuran S, Gazit E, Reches M, Ashkenasy N. Tailor-Made Functional Peptide Self-Assembling Nanostructures. Adv Mater. 2018; 30: 1707083.
24. Tao K, Makam P, Aizen R, Gazit E. Self-assembling peptide semiconductors. Science. 2017; 358: eaam9756.
25. Shigemitsu H, Fujisaku T, Tanaka W, Kubota R, Minami S, Urayama K, Hamachi I. An adaptive supramolecular hydrogel comprising self-sorting double nanofibre networks. Nat Nanotechnol. 2018; 13: 165-72.
26. Black M, Trent A, Kostenko Y, Lee JS, Olive C, Tirrell M. Self-Assembled Peptide Amphiphile Micelles Containing a Cytotoxic T-Cell Epitope Promote a Protective Immune Response In Vivo. Adv Mater. 2012; 24: 3845-49.
27. Chen J, Pompano RR, Santiago FW, et al. The use of self-adjuvanting nanofiber vaccines to elicit high-affinity B cell responses to peptide antigens without inflammation. Biomaterials. 2013; 34: 8776-85.
28. Huang Z-H, Shi L, Ma J-W, et al. A Totally Synthetic, Self-Assembling, Adjuvant-Free MUC1 Glycopeptide Vaccine for Cancer Therapy. J Am Chem Soc. 2012; 134: 8730-33.
29. Rudra JS, Sun T, Bird KC, et al. Modulating Adaptive Immune Responses to Peptide Self-Assemblies. ACS Nano. 2012; 6: 1557-64.
30. Tian Y, Wang H, Liu Y, et al. A Peptide-Based Nanofibrous Hydrogel as a Promising DNA Nanovector for Optimizing the Efficacy of HIV Vaccine. Nano Letters. 2014; 14: 1439-45.
31. Luo Z, Wu Q, Yang C, et al. A Powerful CD8+ T-Cell Stimulating D-Tetra-Peptide Hydrogel as a Very Promising Vaccine Adjuvant. Adv Mater. 2017; 29: 1601776.
32. Wang H, Luo Z, Wang Y, et al. Enzyme-Catalyzed Formation of Supramolecular Hydrogels as Promising Vaccine Adjuvants. Adv Funct Mater. 2016; 26: 1822-29.
33. Yang C, Shi F, Li C, Wang Y, Wang L, Yang Z. Single Dose of Protein Vaccine with Peptide Nanofibers As Adjuvants Elicits Long-Lasting Antibody Titer. ACS Biomater Sci & Eng. 2018; 4: 2000-06.
34. Howland SW, Wittrup KD. Antigen Release Kinetics in the Phagosome Are Critical to Cross-Presentation Efficiency. J Immunol. 2008; 180: 1576-83.
35. Böttcher Jan P, Schanz O, Garbers C, et al. IL-6 trans-Signaling-Dependent Rapid Development of Cytotoxic CD8+ T Cell Function. Cell Rep. 2014; 8: 1318-27.
36. Starbeck-Miller GR, Xue H-H, Harty JT. IL-12 and type I interferon prolong the division of activated CD8+ T cells by maintaining high-affinity IL-2 signaling in vivo. J Exp Med. 2014; 211: 105-20.
37. Bonizzi G, Karin M. The two NF-κB activation pathways and their role in innate and adaptive immunity. Trends Immunol. 2004; 25: 280-88.
38. Hoebe K, Janssen E, Beutler B. The interface between innate and adaptive immunity. Nat Immunol. 2004; 5: 971.
39. Slack E, Hapfelmeier S, Stecher B, et al. Innate and Adaptive Immunity Cooperate Flexibly to Maintain Host-Microbiota Mutualism. Science. 2009; 325: 617-20.
40. Yoshimura S, Bondeson J, Brennan FM, Foxwell BMJ, Feldmann M. Antigen Presentation by Murine Dendritic Cells is Nuclear Factor-kappa B Dependent Both In Vitro and In Vivo. Scand J Immunol. 2003; 58: 165-72.
41. Yoshimura S, Bondeson J, Foxwell BMJ, Brennan FM, Feldmann M. Effective antigen presentation by dendritic cells is NF-κB dependent: coordinate regulation of MHC, co-stimulatory molecules and cytokines. Int Immunol. 2001; 13: 675-83.